



CRITICAL RAW MATERIALS ELIMINATION BY A TOP-DOWN APPROACH TO HYDROGEN AND ELECTRICITY GENERATION

Grant agreement no.: 721065

Start date: 01.01.2017 – Duration: 42 months

Project Coordinator: CNRS

DELIVERABLE REPORT

DELIVERABLE 3.2 – SET OF CRM-FREE ORR CATALYST AND CRM-FREE OR ULTRALOW-PGM HOR CATALYST WITH ACTIVITY VERIFIED BY RDE SENT TO WP5 FOR AEMFC TESTING

Due Date	30/12/2017 (M12)
Author(s)	Frédéric Jaouen, Dario Dekel, Pietro Giovanni Santori, Elena Davydova, Tanja Kallio
Work Package	WP3: Catalyst synthesis and characterization
Work Package Leader	Tanja Kallio (AALTO)
Lead Beneficiary	CNRS
Date released by WP Leader	21/12/2017
Date released by Coordinator	22/12/2017

DISSEMINATION LEVEL

PU	Public	X
PP	Restricted to other programme participants (including the Commission Services)	
RE	Restricted to a group specified by the consortium (including the Commission Services)	
CO	Confidential, only for members of the consortium (including the Commission Services)	

NATURE OF THE DELIVERABLE

R	Report	
P	Prototype	
D	Demonstrator	X
O	Other	

SUMMARY	
Keywords	oxygen reduction reaction, hydrogen oxidation reaction, alkaline media, electrocatalyst, catalyst, critical raw material, platinum group metal
Full Abstract (Confidential)	<p>The report presents activity and stability data for selected electrocatalysts developed during M1-M12 in CREATE for hydrogen oxidation reaction (HOR) and oxygen reduction reaction (ORR) in alkaline medium.</p> <p>For ORR, a Fe-N-C catalyst pyrolyzed in Ar and then NH₃ shows high activity. A restricted activity loss is observed after accelerated-stress-test of electrochemical load cycling in rotating disk electrode. The ORR catalyst reaches the internal CREATE target of activity for Critical Raw Material (CRM)-free catalysts and also passes the internal stability criterion. Composites Fe-N-C/Mn-oxides were also explored for improving peroxide scavenging properties.</p> <p>For HOR, two CRM-free catalysts were developed and one ultralow content Pt-catalyst. As CRM-free, Nickel nanoparticles on a nitrogen-doped carbon support (Ni/N-CNT) and Nickel-Iron nanoparticles on a carbon support (NiFe/C) were developed. Their HOR activity was verified and, while comparable to that reported for other CRM-free catalysts, is yet lower than the internal activity target of CREATE. The 8%Pt/SWNT HOR catalyst very closely approaches the internal CREATE activity target and passes the stability criterion.</p> <p>Approaches to reduce the content of Pt (PGM) and to increase the activity of CRM-free catalysts will be further explored with high throughput methods while the synthesis parameters of CRM-free ORR catalysts will be further refined to reach beyond the state-of-art activities.</p>
Publishable Abstract (If different from above)	

REVISIONS			
Version	Date	Changed by	Comments
1.0	20.11.2017	Frédéric Jaouen (CNRS)	Draft structure
2.0	18.12.2017	Elena Davydova (TECHNION)	HOR catalysts
3.0	19.12	Elena Davydova (TECHNION), Frédéric Jaouen (CNRS), Taneli Rajala (AALTO)	HOR catalysts
4.0	20.12	Tanja Kallio (AALTO)	HOR catalysts



**SET OF CRM-FREE ORR CATALYST AND CRM-FREE OR ULTRALOW-PGM HOR CATALYST WITH ACTIVITY VERIFIED
BY RDE SENT TO WP5 FOR AEMFC TESTING**

CONTENTS

Introduction	4
1. ORR catalyst	5
1.1 Experimental conditions and protocol for ORR activity measurement.....	5
1.2 Experimental conditions and protocol for ORR stability measurement.....	5
1.3 Synthesis of ORR Catalysts	5
1.4 Activity and selectivity of ORR Catalysts	6
1.5 Electrochemical stability of ORR Catalysts	7
1.7 Comparison to internal CREATE targets	8
2. HOR catalysts	10
2.1 Experimental conditions and protocol for HOR activity measurement	10
2.2 Experimental conditions and protocol for HOR stability measurement	11
2.3 Synthesis of HOR catalysts	11
2.3.1 Synthesis of Ni/N-CNT - hydrothermally treated.....	11
2.3.2 Synthesis of NiFe/C – chemically reduced	12
2.3.3 Synthesis of Pt/SWNT with low CRM content	13
2.4 Electrochemical Activity of HOR Catalysts.....	14
2.5 Electrochemical stability of HOR catalysts	15
2.6 Comparison to internal CREATE targets	16
References.....	18



INTRODUCTION

The purpose of D3.2 is to demonstrate the preparation of a first set of CRM-free and low-CRM catalysts developed in CREATE and with significant activity and stability toward the electrode reactions occurring in an alkaline fuel cell, with activity and stability verified in rotating disk electrodes.

In a fuel cell, two electrochemical reactions occur, namely the hydrogen oxidation reaction (HOR) on the anode and the oxygen reduction reaction (ORR) on the cathode. A first set of catalysts for both reactions are demonstrated in the present deliverable, and those catalysts have been transferred to WP5 in sufficient amount for subsequent testing in AEMFC devices with reference commercial AEM membrane from FUMATECH.

Although the ultimate focus of the CREATE project is on the development, for AEMFC devices, of critical raw material (CRM) free catalysts (the list of CRMs as defined by the EU can be accessed at <http://eur-lex.europa.eu/legal-content/EN/ALL/?uri=COM:2017:0490:FIN>, both CRM-free and CRM-lean alternatives are considered in this deliverable for catalyzing the HOR in alkaline medium, as a trade-off between cost and performance. This is necessary as the targeted activity performance for the HOR in alkaline medium is not yet achieved with catalysts that are entirely free of CRM.

Test protocols for the electrochemical activity and durability measurements as well as pass/fail criteria for catalyst intended for each reaction were defined in WP2 (Technical Specifications, Cost Analysis & Life Cycle) of CREATE, and reported in Deliverable 2.1. In the following, the material performance is reflected against these criteria as well as relative to recognized state-of-the-art electrocatalysts for the HOR and ORR in alkaline electrolyte.

1. ORR CATALYST

1.1 EXPERIMENTAL CONDITIONS AND PROTOCOL FOR ORR ACTIVITY MEASUREMENT

The electrochemical experiments were performed with a Biologic SP-300 potentiostat. A three-electrode cell configuration was used for all experiments using 0.1 M KOH as electrolyte solution, a reversible hydrogen electrode as a reference and a graphite plate as counter electrode. As working electrode, the catalyst ink was deposited in a glassy carbon. The catalyst-ink was prepared with 5 mg of non-PGM catalyst in 54 μL of ionomer (Nafion, 5% solution in lower alcohols), 744 μL of ethanol and 92 μL of ultrapure water. The ink was ultrasonicated one hour and the required aliquot was then deposited with a pipet on the glassy carbon, so that a catalyst loading of $0.2 \text{ mg}\cdot\text{cm}^{-2}$ is reached. Once the electrode was completely dry, a drop of water was deposited on it to minimise the entrapment of air bubbles during the immersion of the shaft and RDE-tip in the electrolyte. N_2 was bubbled in the electrolyte for 30 minute, then the cyclic voltammogram in N_2 -saturated electrolyte was recorded by scanning the potential at $10 \text{ mV}\cdot\text{s}^{-1}$ between 0.0 and 1.0 V vs. RHE for a few cycles, until reproducible scans were recorded. The electrolyte was then saturated with O_2 for 30 min, and the polarization measurements from which ORR activity is directly extracted were recorded at a low scan rate of $1 \text{ mV}\cdot\text{s}^{-1}$ in the potential range 0.0-1.1 V vs RHE, and at 1600 rpm rotation rate. It was verified that the scan rate of $1 \text{ mV}\cdot\text{s}^{-1}$ is low enough that capacitive current can be neglected for the investigated catalysts.

1.2 EXPERIMENTAL CONDITIONS AND PROTOCOL FOR ORR STABILITY MEASUREMENT

Accelerated stability tests (AST) were performed by comparison between the initial polarization curve (following the procedure described above) and the polarization curve obtained with the same electrode after 5000 potential cycles between 0.6 and 1.0 V vs. RHE. The 5000 cycles were applied in N_2 -saturated 0.1 M KOH electrolyte, at a scan rate of $100 \text{ mV}\cdot\text{s}^{-1}$ and without any rotation (AST protocol No. 1, as defined in Deliverable 2.1, "Definition of Test Protocols" of the project CREATE). For recording the final polarisation curve, a fresh electrolyte was used, and the same conditions as used for recording the initial polarisation curve were otherwise applied.

1.3 SYNTHESIS OF ORR CATALYSTS

CRM-free Fe-N-C catalyst

The Fe-N-C catalyst was obtained starting from a Zn-based zeolitic imidazolate framework (ZIF-8, Basolite® Z1200, from BASF), 1,10-phenanthroline (phen) and iron acetate. The powder precursors of ZIF-8, phen and ferrous acetate were mixed with low energy ball milling, resulting in a homogeneous catalyst precursor containing 0.5 wt% Fe before pyrolysis. This catalyst precursor was then pyrolyzed in argon at 1050°C for 1 hour, then pyrolyzed in NH_3 at 950°C for 5 min. It is labelled $\text{Fe}_{0.5}\text{-NC}$ (Ar, NH_3).

CRM-free composite Fe-N-C/Mn-oxide

To functionalize Fe-N-C with a co-catalyst that can scavenge hydrogen peroxide during AEMFC operation, various Mn-oxides were screened for their ability to electro-reduce HO_2^- . The Mn-oxide with best combination of peroxide reduction activity and stability was selected, and then physically mixed with $\text{Fe}_{0.5}\text{-NC}$ (Ar, NH_3) in a ratio 20/80 ratio to prepare a composite $\text{Fe}_{0.5}\text{-NC}$ (Ar, NH_3)/ MnO_x .

1.4 ACTIVITY AND SELECTIVITY OF ORR CATALYSTS

The beginning-of-life E vs. I polarization curves measured in RRDE for the two above-described CRM-free ORR catalysts are shown in Fig. 1, lower panel. Also shown is the polarisation curve recorded for a 5%Pt/C catalyst from Johnson Matthey, comprising Pt nanoparticles supported on carbon black. The activity of both CRM-free ORR catalysts is higher than that of 5% Pt/C and their selectivity is comparably low. While the value of the diffusion-limited current density at low potential may give a first indication as to whether the ORR mainly proceeds via a 2 or 4 electron pathway, all 3 catalysts present here a value of diffusion-limited current density that is close to the theoretical value expected for 4 e ORR. To get a more precise insight into selectivity, RRDE measurements were also performed, and the % peroxide measured with this technique is reported in the upper panel of Fig. 1. It confirms the high selectivity of all three catalysts, and also the slight beneficial role played by MnO_x in the $\text{Fe}_{0.5}\text{-NC (Ar, NH}_3\text{)}/\text{MnO}_x$ composite. The latter shows lower % peroxide than $\text{Fe}_{0.5}\text{-NC (Ar, NH}_3\text{)}$ at potentials below 0.55 V vs. RHE, and also lower peroxide release than 5%Pt/C.

The Tafel representation of the same polarization curves but after correction for O_2 diffusion limitation is shown in Fig. 2. The Tafel plot more precisely show the lower activity of the composite relative to the pure Fe-N-C catalyst. While the onset for ORR is similar, the activity or Tafel slope is modified for the composite, possibly due to some surface coverage of Fe-N-C by MnO_x particles, decreasing the accessible number of Fe-based active sites by electrolyte or adding a mass-transport barrier to the most active ORR sites. The Tafel slopes are *ca* 65 mV/decade for 5%Pt/C and 57 mV/decade for $\text{Fe}_{0.5}\text{-NC (Ar, NH}_3\text{)}$ at high potential.

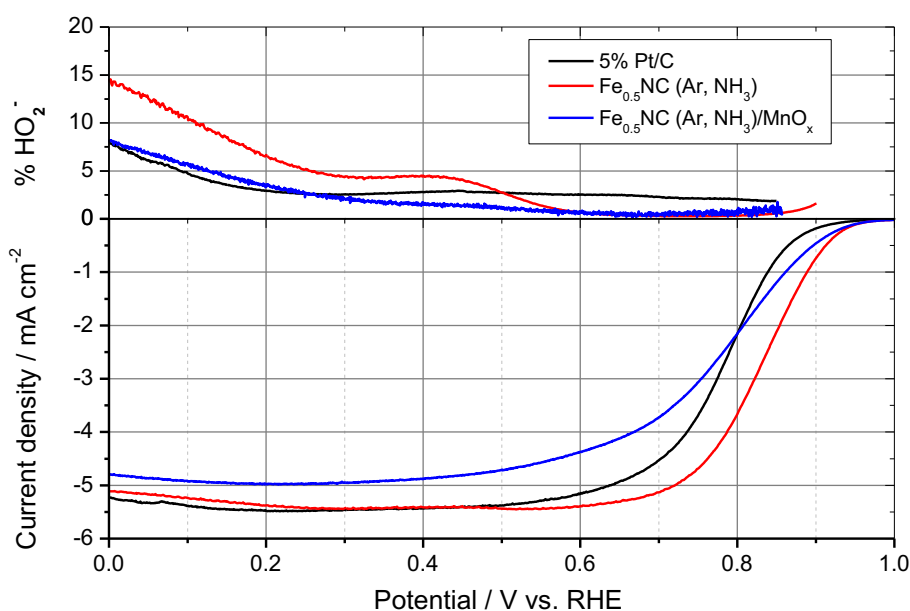


Figure 1: Initial ORR polarization curves measured with RRDE at 1600 rpm for the two CRM-free ORR catalysts and for a reference Pt/C catalyst, measured immediately after break-in. Scan rate $1 \text{ mV}\cdot\text{s}^{-1}$, 0.1 M KOH , room temperature, catalyst loading (mass of all chemical elements) $200 \mu\text{g cm}^{-2}$ on glassy carbon RDE tip. Ionomer binder Nafion.

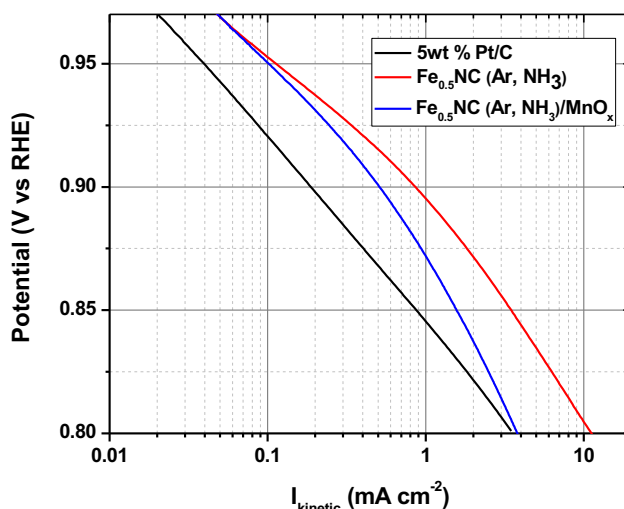


Figure 2: Tafel representation of the initial ORR polarisation curves, extracted from the data shown in Fig. 1.

1.5 ELECTROCHEMICAL STABILITY OF ORR CATALYSTS

The results of the electrochemical AST protocol for ORR that was described in 1.2 are shown in Fig. 3. The curves show only minor changes, mostly related to changes in the diffusion-limited current densities, which may arise due to changes in selectivity of the catalysts. The kinetic current density at 0.9 V (and above) only decreased slightly. The initial ORR current densities achieved at 0.9 V vs. RHE are summarized in Table 1.

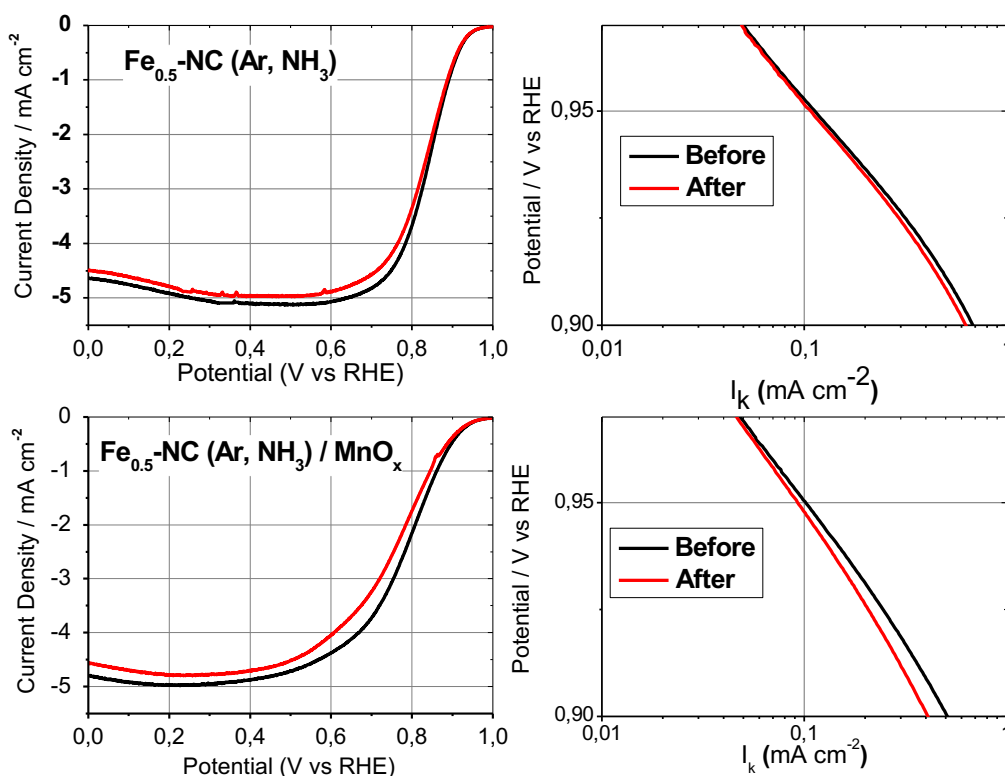


Figure 3: Stability of CRM-free ORR catalysts. Left handside: Polarization curves before (black curve) and after (red curve) 5000 cycles in the range 0.6-1.0 V vs RHE. Right handside: the corresponding Tafel plot presentations.

1.6 COMPARISON TO INTERNAL CREATE TARGETS AND STATE-OF-ART CATALYSTS

Table 1 summarises the initial activity at 0.9 V vs. RHE of the two selected CRM-free catalysts developed in CREATE during months M1-M12 and the internal pass/fail activity criterion defined in D2.1 for transfer into AEMFC. Both these selected CRM-free catalysts pass the initial activity criterion, however only with a small margin. Further optimisation is ongoing to increase the activity, which could allow us decreasing the cathode thickness of AEMFC and thereby improve the prospects for high transport of reactants at high current density. The ORR activity of these catalysts is comparable or higher to state of the art Metal-NC catalysts. At 0.9 V on the Tafel plots, the kinetic current density is 0.5-0.7 mA cm⁻², resulting in mass activity of 2.5-3.5 A/g. This mass activity at pH 13 is very close to some of the best reported activities of FeNC catalysts at 0.9 V, e.g. 7.5 A/g [1], 7.3 A/g [2]. Yamauchi et al. reported a highly ordered mesoporous Fe_{0.25}-N-C catalyst, dodecahedral crystals englobed in particles. The system was obtained by aqueous treatment followed by pyrolysis in N₂ and NH₃ showing high activity of 1.42 mA cm⁻² at 0.9 V (mass activity of 7.1 A/g).[3] Durability test showed a loss of 22.3 mV, indicating a lower stability than for the present FeNC catalyst. Atanassov et al reported three different Fe-N-C catalysts obtained using sacrificial support method.[4] Heat treatment at 975 °C for 45 min in N₂ first and then in NH₃ were applied. Different precursors were used for the three catalysts, with a total amount of ~1% wt of Fe. The best catalyst showed an activity at 0.9 V of 1.41 mA cm⁻², which means a mass activity of 2.3 A/g.

Optimisation of CRM-free ORR catalysts is ongoing, focusing on pyrolysis duration, Fe content and bimetallic catalysts to further improve the activity.

Table 2 summarises the AST stability result, reported as "mV lost during 5000 cycles", at a fixed current density on the polarisation curve. For ORR, the fixed current density was chosen to be -1 mA cm⁻² (where the curve is almost entirely controlled by electrokinetics). Table 2 shows that both CRM-free catalysts passed the stability test, although the composite catalyst shows more loss than the Fe-based only catalyst. This may be due to some Mn leaching from MnO_x during the cycles. Longer stability tests will be performed in the near future, as well as intermediate ORR-activity measurements. This will also be coupled to online detection of metal leaching (Fe or Mn), and also post-AST determination of metal content leached in the electrolyte.

Table 1: Current density values reported at fixed potential for various Fe-N-C catalysts before and after AST No. 1.

CRM-free ORR Catalyst	Initial current density @ 0.9 V vs. RHE / mA·cm ⁻²	Internal pass activity criterion for transfer to AEMFC (*)
Fe _{0.5} -NC (Ar,NH ₃)	0.683	0.50
Fe _{0.5} -NC (Ar,NH ₃)/MnO _x	0.5105	0.50

(*) at a catalyst loading of 200 µg·cm⁻² or less, and with a Tafel slope of 60 mV/decade.

Table 2: Loss of cathode potential at fixed current density of -1 mA cm^{-2} before/after AST No 1 (5000 cycles between 0.6 and 1.0 V vs RHE)

CRM-free ORR Catalyst	Change in cathode potential before/after AST No 1 (read at 1 mA cm^{-2} on diffusion-corrected polarisation curve)	Internal pass stability criterion for transfer to AEMFC (*)
$\text{Fe}_{0.5}\text{-NC (Ar,NH}_3\text{)}$	- 4.5 mV	-40
$\text{Fe}_{0.5}\text{-NC (Ar,NH}_3\text{)/MnO}_x$	- 17.1 mV	-40

2. HOR CATALYSTS

2.1 EXPERIMENTAL CONDITIONS AND PROTOCOL FOR HOR ACTIVITY MEASUREMENT

Nickel-based CRM-free catalysts

10 mg of the CRM-free Nickel-based catalyst is ultrasonically suspended in a mixture of 1.5 ml isopropyl alcohol, 0.35 ml milli-Q water and 0.15 ml of 1 wt % Nafion suspension (prepared by diluting a 10 wt % commercial Nafion suspension in alcohol with the required aliquot of milli-Q water) for 1.5 h. The catalyst/Nafion weight ratio is 85/15. An aliquot of 8 μl of the suspension is applied to a glassy-carbon RDE tip (0.2 cm^2) and dried in air at ambient temperature, resulting in a catalyst loading of $200\text{ }\mu\text{g}\cdot\text{cm}^{-2}$. Before immersing into the electrolyte (1 M KOH at $25\text{ }^\circ\text{C}$), the working electrode is dipped into hot milli-Q water in order to hydrophylize the catalytic layer. The electrochemical measurements were fulfilled according to the following protocol. Hydrophylized electrode is immersed into the electrolyte pre-purged by H_2 at the flow rate of 200-250 mL/min. Open circuit potential is measured versus the reference electrode Hg/HgO/1 M KOH. The HOR polarization curves are registered by scanning the potential between $-0.925\text{ V vs. Hg/HgO}$ to -0.5 V vs. Hg/HgO (0 to $+0.4\text{ V vs. RHE}$) at the scan rate of $1\text{ mV}\cdot\text{s}^{-1}$ and rotation rate of 1100 rpm. The measurements are completed by registering cyclic voltammograms in the electrolyte saturated with N_2 , at the scan rate of $20\text{ mV}\cdot\text{s}^{-1}$ in order to estimate the electrochemically active surface area of metallic nickel.

Low-Pt catalyst

Rotating disk electrode (RDE) experiments for HOR catalysts were performed in 0.1 M KOH at $25\text{ }^\circ\text{C}$, using carbon as counter electrode and RHE as the reference. Catalyst was deposited on a glassy carbon disk of 5 mm diameter, constituting the working electrode. Ink for the deposition was prepared by carefully dispersing catalyst powder in solvent so that pipetting the ink on the working electrode results in a catalyst loading of $200\text{ }\mu\text{g}\cdot\text{cm}^{-2}$ followed by addition of 5 μl of diluted Nafion ionomer solution (50 μl of 5 wt-% Nafion in 2 ml of ethanol).

Before measuring the activity, a break-in procedure was implemented. The dried catalyst layer on the glassy carbon was first contacted with d-water, either by dropping hot deionized-water on top or by immersing the catalyzed RDE tip in a vial with hot milli-Q water ($50\text{-}60\text{ }^\circ\text{C}$). The RDE was then screwed on the rotating shaft and immersed in the electrolyte. Nitrogen was bubbled in the electrolyte for 15-30 min, after which it was directed above the electrolyte, cycling the potential between 0.0 and 0.4 V vs. RHE at $50\text{-}100\text{ mV}\cdot\text{s}^{-1}$ until CVs were reproducible.

For the activity measurement, the electrolyte was saturated with H_2 for about 30 min until OCP stabilized. Polarization curves were measured at $1\text{-}2\text{ mV}\cdot\text{s}^{-1}$ starting from OCP to 0.4 V vs. RHE and back to 0.0 V vs. RHE (only one cycle if positive and negative going scans superimposed, two or more otherwise) at 1600 rpm rotation.

2.2 EXPERIMENTAL CONDITIONS AND PROTOCOL FOR HOR STABILITY MEASUREMENT

The stability of the catalyst material was evaluated using an accelerated stress tests (AST) defined in WP2 (Technical Specifications, Cost Analysis & Life Cycle) of CREATE, and reported in Deliverable 2.1. For the present HOR materials for alkaline medium, AST No. 4 was applied, and is depicted below. The electrode was not rotated during the AST, to avoid particle detachment after prolonged rotation. The catalyst passes the stability test if the potential shift due to the cycling was no more than +40 mV at a given current density.

Table 3: Definition of the AST for HOR catalysts (AST No. 4).

	Electrolyte	Signal shape	Number of cycles	lower / upper potential limits	Scan rate (LSV)
AST 4	N ₂ -satd 0.1 M KOH	LSV	5 000	0.0 / +0.4 V vs RHE	100 mV s ⁻¹

2.3 SYNTHESIS OF HOR CATALYSTS

2.3.1 SYNTHESIS OF Ni/N-CNT - HYDROTHERMALLY TREATED

A hydrothermal method was used to synthesize Ni/N-CNT catalyst. Oxidized multiwall carbon nanotubes (MWCNT) are used as the carbon support. MWCNT are stirred in concentrated H₂SO₄ for 24 h. KMnO₄ is added slowly to the suspension of CNT while stirring, and the mixture is kept under 70 °C for 1 h. The oxidation is completed by slowly adding of concentrated H₂O₂. The oxidized carbon material, CNT_{ox}, is separated by repetitive centrifuging, twice in 5% HCl solution and then in milli-Q water, before drying overnight in a vacuum oven at 90–110 °C. The oxidized CNT is suspended in of isopropyl alcohol. The chemical reduction of NiCl₂ by NaBH₄ is similar to the chemical reduction method, described below. The resultant suspension of Ni/CNT_{ox} placed in the Teflon reactor of autoclave with the addition of N₂H₄×H₂O solution and NH₄OH 25% solution. The mixture is heated up to 150 °C and kept for 3 h under the pressure of 8–10 atm. The catalyst is separated by repetitive centrifuging is dried overnight at 80–90 °C in a vacuum oven.

Figure 4 presents the SEM image of the pristine MWCNT (A) and oxidized MWCNT (B). The figure clearly shows that the morphology of the MWCNT is modified after the oxidation treatment. Figure 5 shows SEM images of hydrothermally treated Ni/N-CNT catalyst, with Ni particles diameter of 20–30 nm. The XRD shows the main peaks of metallic Nickel, with crystal size estimated at 4.4–6.3 nm from Scherrer equation. The elemental composition by XPS is 20.8 at % Ni, 44 at % C, 3.4 at % O and 1.6 at% N.

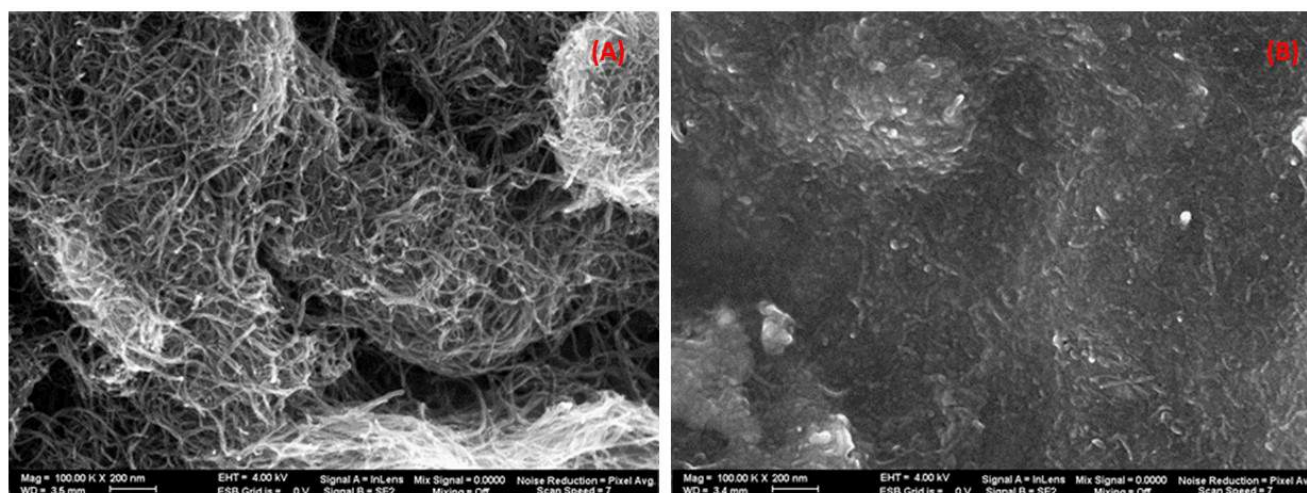


Figure 4: SEM images of (A) pristine MWCNT and (B) oxidized MWCNT. Magnification 100 K. 200 nm scale bar.

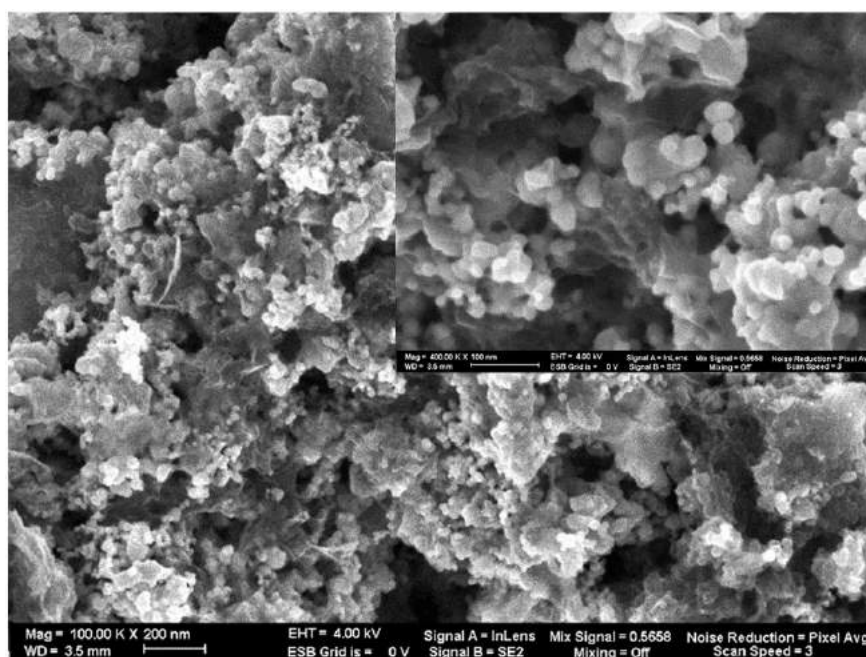


Figure 5: SEM images of Ni/N-CNT catalyst. Magnification 100 K and 400 K (insert). 200 nm scale bar and (insert) 100 nm scale bar.

2.3.2 SYNTHESIS OF NiFe/C – CHEMICALLY REDUCED

A chemical reduction method was used to synthesize NiFe/C catalyst. Carbon black VXCMA22 was ultrasonically suspended in isopropyl alcohol. The solutions of $\text{NiCl}_2 \times 6\text{H}_2\text{O}$ and $\text{FeCl}_2 \times 4\text{H}_2\text{O}$ in milli-Q H_2O each are added to the carbon suspension and ultrasonically dispersed. The resultant suspension and the solution of NaBH_4 in 0.1 M KOH are cooled down in an ice bath. The reduction of metal precursors is carried out in an air-free three-neck flask, placed in the ice-bath, adding cold solution of NaBH_4 drop-wise. The mixture is kept for 2 h before repetitive centrifuging in milli-Q water. The precipitate is dried overnight at 80–90 °C in a vacuum oven. Figure 6 shows SEM images of NiFe/C. The elemental composition by XPS is 2.8 at % Ni, 0.31 at% Fe, 82.5 at % C and 11.8 at % O.

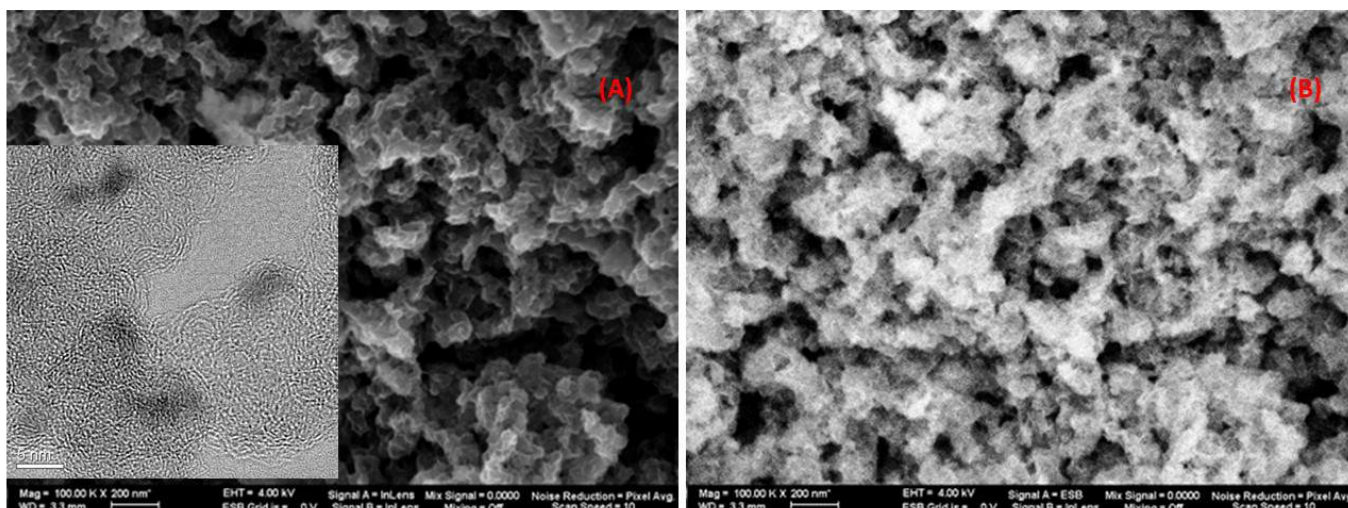


Figure 6: SEM image of (A) NiFe/C catalyst and (B) EsB detected image from the same area. Magnification 100 K. 200 nm scale bar (5 nm scale bar for insert). Light pixels in EsB image (B) are related to a metallic phase.

2.3.3 SYNTHESIS OF Pt/SWNT WITH LOW CRM CONTENT

HOR catalysts with an ultralow amount of Pt on single-wall carbon nanotubes (SWNTs) were prepared by atomic layer deposition (ALD). The pulse lengths of the Pt and oxidizer precursors were varied, which expectedly resulted in improved electrochemical activity for longer pulses. Figure 7 displays the size and distribution of Pt particles on the SWNTs produced by the above-mentioned methods. The weight content of Pt in Pt/SWNT was determined by ICP-MS (JULICH partner) to be 8 wt %.

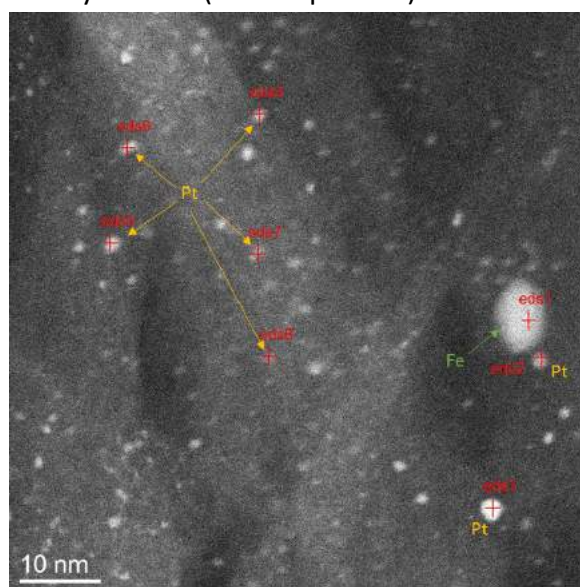


Figure 7: TEM images of the 8 wt % Pt/SWNT catalyst. Particles marked with a red cross have been analysed by EDS. Fe particles are remnants of the catalyst used for the SWNT growth.

2.4 ELECTROCHEMICAL ACTIVITY OF HOR CATALYSTS

Nickel-based CRM-free catalysts

Figure 8A shows the cyclic voltammograms recorded in N_2 -saturated 1 M KOH for Ni/N-CNT while Figure 8B shows the HOR polarization curve recorded in H_2 -saturated 1 M KOH at low scan rate. Figure 9 A and 9B show the same type of results but for the NiFe/C catalyst. The electrochemically estimated surface of metallic nickel is about three times higher for the latter catalyst. However, its HOR activity is slightly lower than that of Ni/N-CNT. The HOR polarization curves show an increase in current density with increase potential up to ca +0.15 V vs. RHE, then a decreasing current with further increase potential. This is assigned to increased surface coverage by nickel hydroxide, decreasing the electrochemical active surface area for HOR on the Ni-based catalysts. The diffusion-limited current density for HOR that would be expected at 1100 rpm (ca 2 mA cm^{-2}) is never reached.

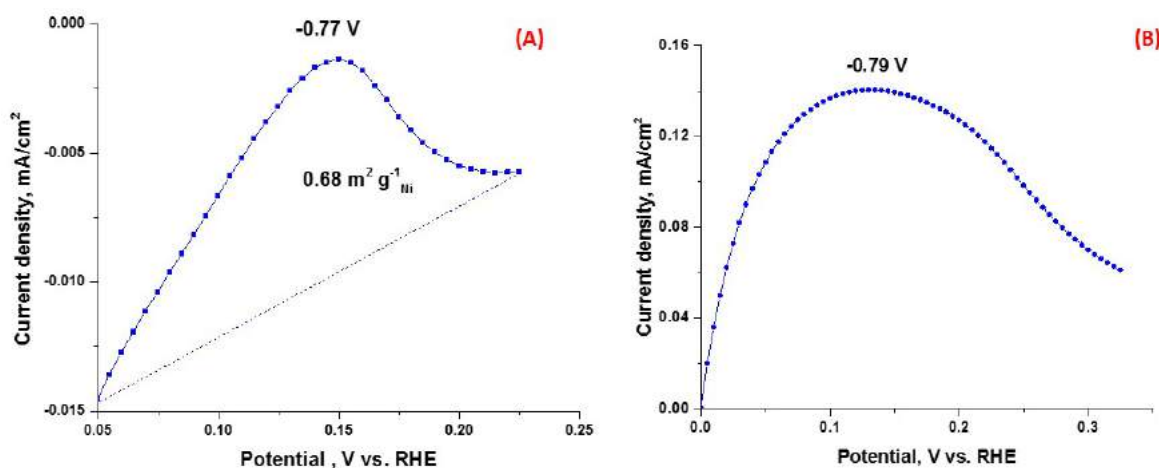


Figure 8: Cyclic voltammogram (A) and HOR polarization curve (B) for Ni/N-CNT catalyst. $200 \mu\text{g} \cdot \text{cm}^{-2}$ catalyst loading, rotation rate 1100 rpm. The numbers indicate the electrochemically estimated area of metallic nickel and the potential at which the peak current density is observed. Nafion ionomer used as a binder.

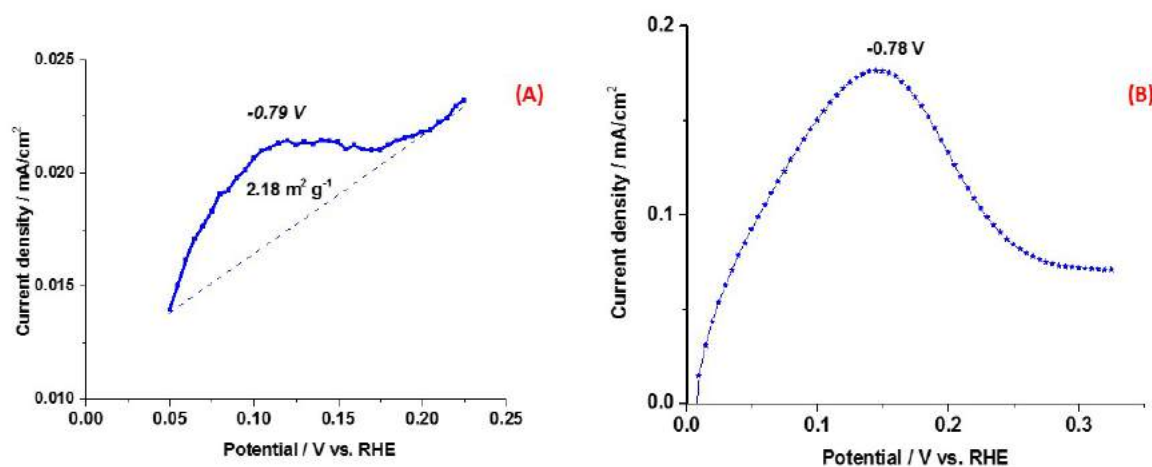


Figure 9: Cyclic voltammogram (A) and HOR polarization curve (B) for NiFe/C catalyst. $200 \mu\text{g} \cdot \text{cm}^{-2}$ catalyst loading, rotation rate 1100 rpm. The numbers indicate the electrochemically estimated area of metallic nickel and the potential (in V vs Hg/HgO) at which the peak current density is observed. Nafion ionomer used as a binder.

Ultralow-Pt catalyst

Figure 10 shows the initial HOR polarisation curve for 8% Pt/SWNT. The curve (a) shows a linear behaviour near the thermodynamic potential for $\text{H}_2\text{O}/\text{H}_2$ (kinetically controlled region), then increases with increasing potential up to the diffusion-limited current expected. Curve (b) is the diffusion-corrected curve extracted from curve (a) with the Koutecky-Levich equation (assuming the HOR reaction rate is proportional to the H_2 concentration). With respect to the Pt mass loading, exchange current density of $0.058 \text{ A/mg}_{\text{Pt}}$ was obtained after Koutecký–Levich and Tafel analyses. The difference with literature value of $0.35 \text{ A/mg}_{\text{Pt}}$ on Pt/C [5] can be diminished by further developing the synthesis. PtRu bimetallic catalyst on SWNT will also be prepared by ALD in the near future, based on the known higher HOR activity in alkaline medium of PtRu vs. Pt.

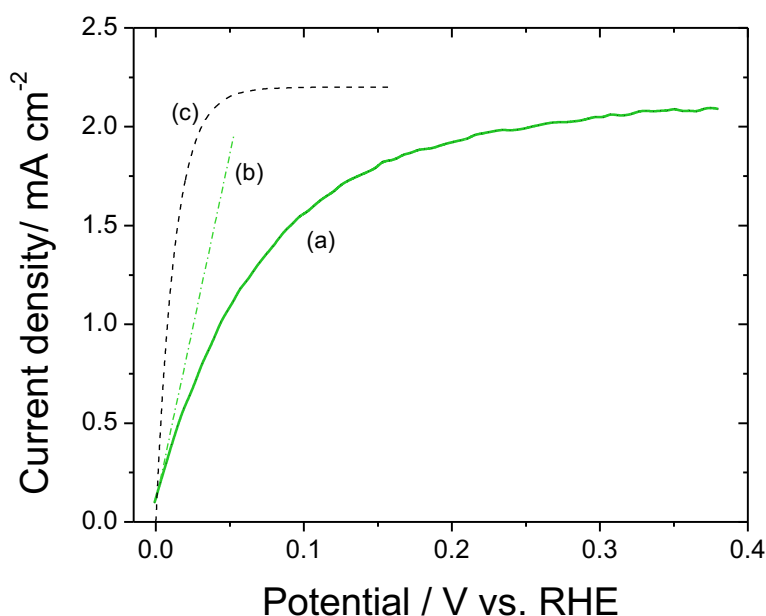


Figure 10: HOR polarization curve for 8 % Pt/SWNT catalyst (a). $200 \mu\text{g} \cdot \text{cm}^{-2}$ catalyst loading ($16 \mu\text{g}_{\text{Pt}} \text{cm}^{-2}$), rotation rate 1600 rpm. The curve (b) represents the curve (a) after correction for H_2 -diffusion limitation with the Koutecky-Levich equation and (c) represents the theoretical curve expected for infinitely fast reaction with concentration overpotential only.

2.5 ELECTROCHEMICAL STABILITY OF HOR CATALYSTS

The stability test result for the Pt/SWNT HOR catalysts prepared in the frame of CREATE is shown in Fig. 11. The initial activity is close to but slightly lower than for the Pt/SWNT electrode in section 2.4, however the activity after AST No 4 is higher than before the AST, demonstrating the stability of 8%Pt/SWNT prepared by ALD to the AST No 4. The stability was expected under those cycling conditions for such a catalyst based on Pt.

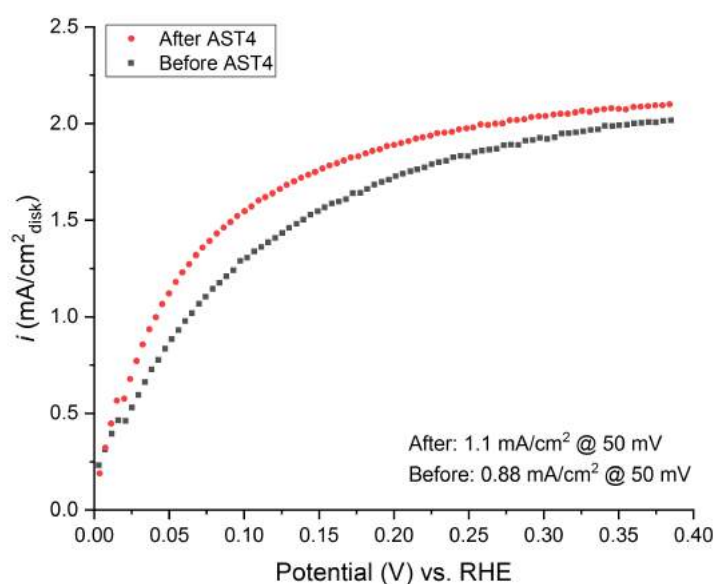


Figure 11: HOR polarization curves before and after the stability test (AST No. 4) in 0.1 M KOH, scan rate 2 mV/s, rotation rate 1600 rpm.

2.6 COMPARISON TO INTERNAL CREATE TARGETS

Table 4 summarizes the HOR kinetic current densities at 0.05 V vs. RHE. Kinetic current densities at that potential were 0.10, 0.11 and 1.88 mA·cm⁻² for NiFe/C, Ni/N-CNT and Pt/SWNT. In other words, at this moment, only Pt/SWNT approaches closely the HOR activity criterion defined for HOR catalysts in CREATE Deliverable 2.1 (2.2 mA·cm⁻² at 0.05 V for catalyst loading of 200 µg·cm⁻² or less). As the performance achieved with these CRM free NiFe/C and Ni/N-CNT do not meet the CREATE targets, in near future Ni based bimetallic catalyst with different compositions will be screened. Furthermore, to achieve the CREATE targets for HOR catalysts, as a parallel approach ultra-low-CRM catalysts with Pd based bi- and trimetallic as well as Pt based bimetallic compounds are investigated.

Table 4: Summary of Nickel surface and electrochemical properties of Pt/SWNT, Ni/N-CNT and NiFe/C catalysts.

Catalyst	Specific surface area of nickel or platinum, m ² /g _{Nickel}	i (at η=0.05 V) ^(*) / mA cm ⁻²
NiFe/C	0.68 m ² /g _{Nickel}	0.10
Ni/CNT-N	2.18 m ² /g _{Nickel}	0.11
Pt/SWNT	NM	1.88 ^(*)
Internal CREATE pass criterion of HOR activity for transfer to AEMFC (at loading of 200 µg·cm ⁻² or less)	--	2.20 ^(*)

(*) corrected for Ohmic drop and H₂ diffusion limitation

Table 5 summarises the stability of Pt/SWNT after AST No 4 (an activity improvement is in fact observed), and the status relative to the pass/fail target of stability for transfer to AEMFC. The table shows that Pt/SWNT passes the HOR stability criterion defined in Deliverable 2.1 (maximum acceptable change in overpotential of +40 mV after AST No. 4).

Table 5: Summary of Pt/SWNT stability after AST No 4 (5000 cycles between 0 and 0.4 V vs RHE at 100 mV/s)

Catalyst	Max. shift in potential at 0.5 mA/cm ² after AST No 4	Pass/fail criterion
8 % Pt/SWNT	-7.5 mV	≤ +40 mV



REFERENCES

- [1] Meng et al, **pH-effect on oxygen reduction activity of Fe-based electro-catalysts**, *Electrochem. Commun.* 11 (2009) 1986-1989
- [2] Kim et al, **The role of pre-defined microporosity in catalytic site formation for the oxygen reduction reaction in iron- and nitrogen-doped carbon materials**, *J. Mater. Chem. A*, 5 (2017) 4199-4206
- [3] Tan H. et al, **Perfectly ordered mesoporous iron-nitrogen doped carbon as highly efficient catalyst for oxygen reduction reaction in both alkaline and acidic electrolytes**, *Nano Energy* 36 (2017) 286-294
- [4] Hossen M. et al, **Synthesis and characterization of high performing Fe-N-C catalyst for oxygen reduction reaction (ORR) in Alkaline Exchange Membrane Fuel Cells**, *J. Power Sources* 375 (2018) 214-221
- [5] Sheng, W. et al., **Hydrogen Oxidation and Evolution Reaction Kinetics on Platinum: Acid Vs Alkaline Electrolytes**, *J. Electrochem. Soc.*, 157.11 (2010): B1529-B1536.